Nigerian Research Journal of Engineering and Environmental Sciences 9(1) 2024 pp. 249-264
p ISSN: 2635-3342; e ISSN: 2635-3350

Nigerian Research Journal of Engineering and Environmental Sciences
Journal homepage: www.rjees.com

Original Research Article

Transport and Diffusion Phenomena Modelling of Some Polycyclic Aromatic Hydrocarbons through the Human Skin

***[1]Odisu, T. and [2]Oboh, I.**

[1]Department of Petrochemical Engineering, Federal University of Petroleum Resources, Effurun, Nigeria.
[2]Department of Chemical Engineering, University of Uyo, Uyo, Nigeria.
*odisu.teddy@fupre.edu.ng

http://doi.org/10.5281/zenodo.12599688

ARTICLE INFORMATION

Article history:
Received 27 Mar. 2024
Revised 24 Apr. 2024
Accepted 10 May. 2024
Available online 30 Jun. 2024

Keywords:
Polycyclic aromatic hydrocarbon
Skin
Model
Vehicle
Stratum corneum
Epidermis
Dermis

ABSTRACT

Polycyclic aromatic hydrocarbons (PAHs) are of environmental and public health concerns and contribute to adverse skin aging and pigmentary disorder. For a better understanding of the transport characteristics of the human skin, transient state predictive mathematical models were successfully developed for the evaluation of the rate of transport of some selected polycyclic aromatic hydrocarbons through the human skin. Based on existing empirical relations and relevant assumptions, correlations were derived to evaluate the transdermal diffusive properties such as the diffusion coefficient, rate of evaporation and rate of elimination of organic compounds at the different layers of the skin. The developed computer-based models were solved using computational fluid dynamics. The simulation of the rate of transport for toluene, naphthalene, fluorine and anthracene were carried out for a duration of 20 hours through the three layers of the fore arm skin of an adult male under different operating conditions. The result indicated $7.234e^{-3}\ kg/m^3$, $5.341e^{-3}\ kg/m^3$, $2.854e^{-3}\ kg/m^3$, *and* $1.310e^{-2}\ kg/m^3$, *respectively. From the derived models the stratum corneum showed the highest degree of resistance to transdermal transport of chemicals when compared with other layers of the skin, which is in accordance with literature. Risk analysis were performed for all the compound and their health effects observed. Sensitivity analysis was also carried out on all the estimated parameters and the stratum corneum was shown to be the most sensitive section.*

1. INTRODUCTION

The skin is the body's largest protective organ and first line of defense against toxicant exposure. The exposure of the skin to chemicals with toxic potency in the workplace has become an important issue in industrial and regulatory toxicology. Of particular concern is the exposure to crude oil and associated petroleum hydrocarbon components. Exposure of the skin to crude oil and other petroleum products can lead

to a variety of skin reactions with varying intensity ranging from skin dryness, skin irritation to irreversible skin changes such as skin tumors (Saranya et al, 2020). Skin irritation can cause a broad range of sensory and visible effects including dryness, fissuring, erythema, and oedema, which occur as a result of local inflammatory processes following single or repeated contact of the skin with chemicals (Almad et al, 2021; Saranya et al., 2020).

The structure of the skin is highly organized and multi-layered. The skin is broadly considered to be composed of two layers: The epidermis, which is a nonvascular layer of approximately 100 μm thick; and the highly vascularized dermis of about 500 μm to 3,000 μm thick. The layer thought to provide the major barrier to adsorption and absorption of most substances deposited on the skin surface is the outermost layer of the epidermis, which is the stratum corneum and it is about 10-40 μm thick (Dancik et al, 2013).

When pollutants such as components of crude oil like polycyclic aromatic hydrocarbons are is allowed to contact the skin, various mass transfer processes such as adsorption, absorption, evaporation, diffusion, etc., come into play as these compounds are transported through the various layers of the skin (Laurent, 2022)

Skin (percutaneous, dermal) absorption is the transport of chemicals from the outer surface of the skin into the body. It is a route of exposure for toxic substances. However, the assessment of the effect will require an understanding and analysis of the percutaneous absorption kinetics which can be obtained through experiments. But for a multicomponent mixture like crude oil, this may be impractical. Modelling of percutaneous transport provides an ethical and viable alternative to laboratory experimentation (Jane and Jane, 2003; Neha et al., 2017). More reliable mathematical models for predicting dermal absorption can save a great deal of effort compared to experimentally determining absorption rates for the thousands of potentially hazardous chemicals or components individuals may be exposed to on a daily basis.

Over the years, there have been conscious efforts toward the development of predictive mathematical models for dermal transport of drugs and some chemicals through the skin (Rania et al., 2012; Dominik et al., 2015; Won et al., 2021; Lee et al., 2022). However, there is a dearth of such models for specific petroleum hydrocarbon components particularly the aromatics. Specific attention is required in this direction because, in areas where crude oil is produced, there are very high possibilities of dermal contact arising from routine operations like sampling operations and maintenance. Other situations that can lead to crude oil contact include oil spill management (arising from natural phenomenon, equipment and transport line failure, disposal or human intervention), abandoned oil spill sites where the producing companies or the relevant body saddled with the responsibility to manage specific oil spill in specific areas has refused to take responsibility, thus opening a window for locals to contact the spilled oil as in the case with some areas of Nigerian Niger Delta. Therefore, the need to develop mathematical model for cyclic aromatic hydrocarbon dermal transport in the human skin is more than important. This will provide a means of predicting the possible evaluation and expected damage in case of contact before such occurs and a basis for contingency arrangement in the management of such occurrence.

Hence, the aim of this work is to develop predictive mathematical models and also simulate using computational fluid dynamics approach in solving same for the evaluation of the rate of transport of polycyclic aromatic hydrocarbons through human skin. The models developed, and solutions obtained will provide good description of the transport pattern of these polycyclic aromatic hydrocarbons (PAHs) studied through the human skin. It will enable effective dermal risk assessment for whole PAHs.

2. METHODOLOGY

2.1. Model Development

The general Conservation equation expressed in Equation 1 serves as the basis for modelling the rate of transport of PAHs on human skin (Dominik et al, 2015). The model development considers the vehicle and the three layers of the skin; Stratum corneum (sc), viable epidermis (ve) and dermis (de) as shown in Figure 1. Each layer has a representative thickness (hi), Diffusion coefficient (Di) and partition coefficient with respect to the vehicle (Ki). In addition, there is a first-order rate of clearance in the dermis representing the systemic absorption by the skin capillaries, nerves and blood.

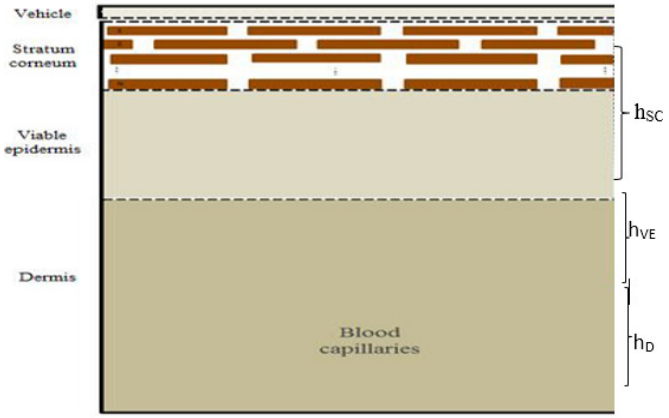

Figure 1: Different layers and vehicle of the skin

To effectively develop the models and obtain the relevant responses, the following assumptions were made:

i. diffusion occurs in two-dimensions;
ii. mass transfer is mainly based on diffusion, and as such, convective fluid flow is negligible;
iii. no reaction or metabolism of solute;
iv. no generation of solute;
v. depletion or sink of solute in the vehicle is due to evaporation of solute;
vi. demis is homogenous;
vii. consumption is by first order reaction;
viii. there is clearance or consumption of solute by blood in the dermis;
ix. flow is accounted for by the sink term in the dermis;
x. dermis and blood grid are in equilibrium.

$$\frac{\partial C_{A[V]}}{\partial t} + \mathrm{U}\left[\frac{\partial C_{A[V]}}{\partial \mathrm{x}} + \frac{\partial C_{A[V]}}{\partial \mathrm{y}} + \frac{\partial C_{A[V]}}{\partial \mathrm{z}}\right] = D_{A[V]}\left[\frac{\partial^2 C_{A[V]}}{\partial x^2} + \frac{\partial^2 C_{A[V]}}{\partial y^2} + \frac{\partial^2 C_{A[V]}}{\partial z^2}\right] + R_{A[V]} \quad (1)$$

where;

$C_{A[V]}$ represents the concentration of the crude oil or a specific crude oil component in the vehicle

$\frac{\partial C_{A[V]}}{\partial t}$ is the transient term

$\mathrm{U}\left[\frac{\partial C_{A[V]}}{\partial \mathrm{x}} + \frac{\partial C_{A[V]}}{\partial \mathrm{y}} + \frac{\partial C_{A[V]}}{\partial \mathrm{z}}\right]$ represents the convection term

$D_{A[V]}\left[\frac{\partial^2 C_{A[V]}}{\partial x^2} + \frac{\partial^2 C_{A[V]}}{\partial y^2} + \frac{\partial^2 C_{A[V]}}{\partial z^2}\right]$ is the diffusion term

$R_{A[V]}$ represents the source or sink term

Based on the assumptions made above, the convective mass transfer term is ignored and the transport equation becomes;

$$\frac{\partial C_{A[V]}}{\partial t} = D_{A[V]}\left[\frac{\partial^2 C_{A[V]}}{\partial x^2} + \frac{\partial^2 C_{A[V]}}{\partial y^2}\right] + R_{A[V]} \quad (2)$$

For an effective modeling, the three sections including the vehicles were considered.

2.1.1. Vehicle

The vehicle is the first section to be considered in this modeling. The diffusion coefficient of the vehicle is estimated using the Stokes-Einstein's equation (Ibrahim and Kasting, 2010)

$$D_{A[V]} = \frac{K_c T}{6\pi\mu R_S} \tag{3}$$

where

K_c is the Boltzmann constant; given as $1.38054 \times 10^{-23}\ J/K$

T is the absolute temperature of the medium

μ is the viscosity of the vehicle

R_S is the raduis of the solute

And R_S is given by

$$R_S = \sqrt[3]{3/4\,(0.9087\ MW)} \tag{4}$$

Therefore $D_{A[V]}$ becomes;

$$D_{A[V]} = \frac{1.38054\times10^{-23}.T}{6\pi\mu\left(\sqrt[3]{3/4(0.9087\ MW)}\right)} \tag{5}$$

The rate of evaporation (sink term) depends on (i) the volatility of the compound (ii) the size of the spill (iii) the temperature of the surrounding area (iv) the wind speed

The rate of evaporation is therefore given by Equation 6;

$$R_{A[V]} = \frac{k_{evap}.\rho}{h_V} \tag{6}$$

Dancik,et al., 2013, gave the physio-chemical correlation highlighted in Equation 6 for the numerical estimation of the evaporation rate constant $k_{evap}.\ \rho$ as;

$$k_{evap}.\rho = k_g \frac{MW.P_{VP}}{0.76RT} \tag{7}$$

where MW is the Molecular weight of the solute in μg/mol, P_{VP} is the Vapour Pressure in Torr, ρ is the pure compound density in $\mu g/cm^3$, T is the absolute temperature, h_V thickness of the spill in cm, R is the gas rate constant (0.0821 L atm deg^{-1}mol^{-1}) and k_g is the gas phase mass transfer coefficient

US_EPA, 1981; Kasting and Miller, 2006 , developed the empirical correlation shown in Equation 8 for estimating k_g

$$k_g = 6320\frac{u^{0.78}}{MW^{1/3}} \tag{8}$$

where u is the wind velocity

The rate of evaporation ($kg/m^3.s$) becomes:

$$R_{A[V]} = 2.778 \times 10^{-7} \left(\frac{(101288.67)(\frac{u^{0.78}.MW^{2/3}.P_{VP}}{T})}{h_V} \right) \quad (9)$$

Therefore, from Equation 2, the overall mass transfer equation in the vehicle is now given by;

$$\frac{\partial C_{A[V]}}{\partial t} = \left(\frac{1.38054\times10^{-23}.T}{6\pi\mu\left(\sqrt[3]{3/4(0.9087\ MW)}\right)} \right) - 2.778 \times 10^{-7} \left(\frac{(101288.67)(\frac{u^{0.78}.MW^{2/3}.P_{VP}}{T})}{h_V} \right) \quad (10)$$

2.1.2. Stratum corneum

As in the case of the vehicle, Equation 1 was applied in modelling the mass transfer in the stratum corneum and the necessary parameters were evaluated.

The diffusion coefficient was estimated using Equation 11 (Crank, 1975)

$$\text{Dsc} = \frac{K_P.h_{SC}}{K_{SC/V}} \quad (11)$$

where $K_{sc/v}$ is the partition coefficient between Stratum Corneum and adjacent solution, h_{sc} is the Stratum Corneum thickness (or diffusion length) and K_P is the permeability coefficient of the stratum corneum

To apply Equation 11, the partition coefficient using octanol/water partition coefficient, (Ko/w) (Chen,et al., 2015) was determined by assuming the vehicle to be water.

According to Equation 12, the partition coefficient of the stratum cornium with water as the vehicle is given as a sum of that of the lipid –water and the corneocytes-water expressed as Equation 12;

$$k_{\text{sc/w}} = 0.0927 * \left(0.43\left(log_{o/w}\right)^{0.81}\right) + 0.9073 * \left(\frac{0.9*\left(0.54\left(log_{o/w}\right)^{0.27}\right)+0.6}{0.9*(1/1.37)+0.6} \right) \quad (12)$$

If the non-volatile vehicle is not pure water, then the stratum corneum to vehicle partition coefficient is given by (Chen, et al., 2010):

$$k_{\text{sc/v}} = \frac{0.0927*\left(0.43\left(log_{o/w}\right)^{0.81}\right)+0.9073*\left(\frac{0.9*\left(0.54\left(log_{o/w}\right)^{0.27}\right)+0.6}{0.9*(1/1.37)+0.6} \right)}{S_V/S_W} \quad (13)$$

Also, Potts and Guy model (Fu et al., 2004) was adopted for the permeability of hydrocarbons through the stratum corneum being the most cited empirical model for permeability of compounds as shown in Equation 14.

$$Log\ K_P = \text{-}6.3 + 0.71.Log\ K_{O/W} - 0.0061MW \quad (14)$$

where K_P is the permeability coefficient expressed in cm/s and $K_{O/W}$ is the octanol/water partition coefficient.

Imputing the empirical relations for each of the unknowns, the diffusion coefficient for the stratum corneum can be estimated using the Equation 15 and by substitution of Equations 12 and 13 into Equation 11. Hence;

$$\mathrm{Dsc} = \frac{10^{-6.3+\,0.71.LogK_{O/W}-0.0061.MW}.\mathrm{h_{sc}}}{\left(\frac{0.0927*\left(0.43\left(logk_{O/W}\right)^{0.81}\right)+0.9073*\left(\frac{0.9*\left(0.54\left(logk_{O/W}\right)^{0.27}\right)+0.6}{0.9*(1/1.37)+0.6}\right)}{S_V/S_W}\right)} \tag{15}$$

The stratum corneum thickness varies with the site of application. Therefore,

$$\frac{\partial \mathrm{C_A}}{\partial \mathrm{t}} = \frac{10^{-6.3+\,0.71.\mathrm{Log\ K}-0.0061.\mathrm{MW}}.\mathrm{h_{sc}}}{\left(\frac{0.0927*\left(0.43\left(\mathrm{logk_{o/w}}\right)^{0.81}\right)+0.9073*\left(\frac{0.9*\left(0.54\left(\mathrm{logk_{o/w}}\right)^{0.27}\right)+0.6}{0.9*\left(1/1.37\right)+0.6}\right)}{\mathrm{S_V/S_W}}\right)}\left[\frac{\partial^2 \mathrm{C_A}}{\partial \mathrm{x}^2}+\frac{\partial^2 \mathrm{C_A}}{\partial \mathrm{y}^2}\right] \tag{16}$$

2.1.3. Viable epidermis

The viable epidemis is the skin layer just beneath the stratum corneum. According to Lee and Hwang, (2002), it has an average thickness of 100 μm. In modelling the transport of hydrocarbons through the viable epidemis, the fundamental governing equation expressed in Equation 1 and the assumptions there-off were applied. In line with the pattern established, the diffusion coefficient and partition coefficient of the viable epidermis were evaluated first. The partition coefficient was calculated from the equation proposed by Kretsos, et al., 2008, and later modified by Ibrahim and Kasting, 2010 as shown in Equation 17.

$$\mathrm{K_{VE}} = 0.7\ (0.68\ + \frac{0.32}{F_U} +\ 0.025\ F_{\mathrm{NON}} K_{O/W}) \tag{17}$$

While the diffusion coefficient of the viable-epidermis was gotten from the Equation 18.

$$D_{(A)VE} = \frac{10^{-8.15-0.655LogMW}}{(0.68+\frac{0.32}{F_U}+\ 0.025\ F_{\mathrm{NON}} K_{O/W})} \tag{18}$$

Hence Equation 2 can be re-written to give;

$$\frac{\partial C_{A(VE)}}{\partial t} = D_{(A)VE}\left[\frac{\partial^2 C_{A(VE)}}{\partial x^2}+\frac{\partial^2 C_{A(VE)}}{\partial y^2}\right]$$

and by substitution from Equation 18, this becomes;

$$\frac{\partial C_{A(VE)}}{\partial t} = \left(\frac{10^{-8.15-0.655LogMW}}{0.68+\frac{0.32}{F_U}+\ 0.025\ F_{\mathrm{NON}} K_{O/W}}\right)\left[\frac{\partial^2 C_{A(VE)}}{\partial x^2}+\frac{\partial^2 C_{A(VE)}}{\partial y^2}\right] \tag{19}$$

2.1.4. Dermis

The dermis is a thick and elastic layer located beneath the epidermis and is comprised largely of fibroblasts and collagen. This layer hosts a network of capillary blood vessels as well as nerve fibres (Richard, 2012). The average thickness of the dermis is reported to be around 1000 μm (Lee and Hwang, 2002)

Adopting Equation 1 as the fundamental governing equation and applying the assumptions previously made, the new look equation becomes Equation 20.

$$\frac{\partial C_{A(D)}}{\partial t} = D_{A(D)}\left[\frac{\partial^2 C_{A(D)}}{\partial x^2}+\frac{\partial^2 C_{A(D)}}{\partial y^2}\right] - K_E C_{A(D)} \tag{20}$$

Where $K_E C_{A(D)}$ is the elimination rate of compound from the dermis by blood and nerves clearance.

The diffusion coefficient and partition coefficient have similar empirical correlations with those of the viable epidermis (Mccarley and Bunge, 2001). Deeper layers, including the viable epidermis and dermis, are often lumped together and treated as a homogeneous layer (Mccarley and Bunge, 2001) which has been shown to be adequate for many permeants (Scheuplein and Bronaugh, 1983). Partition coefficients in the dermis was investigated (Rania et al., 2012) and given as:

$$\mathrm{K}_{A(D)} = 0.7\ (0.68\ + \frac{0.32}{F_U} +\ 0.025\ F_{\mathrm{NON}} K_{O/W}) \tag{21}$$

The diffusion coefficient of the dermis is based on its binding/partitioning properties and is given from the equation below:

$$D_{A(D)} = \frac{10^{-8.15-0.655 LogMW}}{(0.68 + \frac{0.32}{F_U} + 0.025\ F_{\mathrm{NON}} K_{O/W})} \tag{22}$$

Below the dermis lies a vast connection of nerves and blood capillaries to which the diffusing is taken from the dermis. This is termed as clearance. Partitioning of solute into blood capillaries of the dermis and its subsequent convective transport and partitioning back into the tissue could also significantly contribute to the spatial transport of the solute.

The elimination rate $\mathrm{K_E}$ can be estimated from Equation 23:

$$K_E = \frac{F_{Ud} Q_B PS}{(Q_B + F_{Ud} PS)} \tag{23}$$

Where F_{Ud} is the fraction of unbound (to albumin) solute, PS is the permeability surface area and Q_B is the volumetric blood flow rate.

The volumetric blood flow of the skin Q_B can be estimated according to cardiac output. The average resting cardiac output is $9.52 * 10^{-5}\, m^3/s$ and $8.33 * 10^{-5}\, m^3/s$ for a human male and female, respectively (Carroll and Abdel-Rahman, 2007). The overall blood flow to the skin, is estimated to be 5% of cardiac output (Rania et al., 2012). Therefore, the overall skin blood flow is given as $4.76 * 10^{-6}\, m^3/s$ for male and $4.165 * 10^{-6}\, m^3/s$ for female. Blood flow is assumed to have uniform distribution in the dermis.

The permeability surface area is given as the octanol-water permeability coefficient $log_{o/w}$ (Anissimov and Roberts, 2011)

$$PS = 10^{log k_p} \tag{24}$$

$$PS = 10^{-6.3\ +\ 0.71 . Log\ K_{O/W} - 0.0061 . MW} \tag{25}$$

Therefore, Equation 22 becomes

$$K_E = \frac{F_{Ud} Q_B \left(10^{-6.3\ +\ 0.71 . Log\ K_{O/W} - 0.0061 . MW}\right)}{(Q_B + F_{Ud} \left(10^{-6.3\ +\ 0.71 . Log\ K_{O/W} - 0.0061 . MW}\right)} \tag{26}$$

The overall transfer equation:

$$\frac{\partial C_{A(D)}}{\partial t} = \left(\frac{10^{-8.15-0.655 LogMW}}{(0.68 + \frac{0.32}{F_{Ud}} + 0.025\ F_{\mathrm{NON}} K_{O/W})}\right)\left[\frac{\partial^2 C_{A(D)}}{\partial x^2} + \frac{\partial^2 C_{A(D)}}{\partial y^2}\right] - \left(\frac{F_{Ud} Q_B \left(10^{-6.3\ +\ 0.71 . Log\ K_{O/W} - 0.0061 . MW}\right)}{(Q_B + F_{Ud} \left(10^{-6.3\ +\ 0.71 . Log\ K_{O/W} - 0.0061 . MW}\right)}\right) C_{A(D)} \tag{27}$$

2.1.5. Initial and boundary conditions

The concentration in the stratum corneum is a function of distance in the x and y directions, and time i.e. $C(x,y,t)$. The initial concentration of the compound C_0 is the concentration of the solute in the vehicle. At time (t) equals zero, the concentration of solute at any part in the skin is zero. As there is no solute initially present in the stratum corneum, viable epidermis and dermis.

$$C_A(x,y,0) = 0 \tag{28}$$

The boundary conditions are considered for each of the sides of the framework, i.e. left, right top and bottom.

- **Left and Right boundary**

  There is a No-Flux condition on the left and right boundary of the skin

  $$\frac{\partial C}{\partial x}|(x = 0, y, t) = 0 \tag{29}$$

  $$\frac{\partial C}{\partial x}|(x = x_n, y, t) = 0 \tag{30}$$

- **Top boundary**

  There is no outward flux from the vehicle to the atmosphere

$$\frac{\partial C}{\partial y}|(x, y = 0, t) = 0 \tag{31}$$

- **Bottom boundary**

  The condition at the bottom boundary, there is a total sink condition

  $$C_A(x, y = h_D, t) = 0 \tag{32}$$

2.2. Input Parameters for Different Body Sites

In a bid to solve the models developed, input parameters were sourced from exiting literatures as shown in Table 1. These parameters were inputted appropriately and the results obtained thereafter are discussed in the next section.

Table 1: Model geometrical input parameters for different body sites.

Body site	Stratum corneum (μm)	Viable epidermis (μm)	Dermis (μm)
Chest	14.80	98.5	1337
Forearm	12.98	102.1	1077
Abdomen	14.52	79.4	1248
Scalp	14.36	93.6	788
Back	14.39	76.8	1941
Thigh	12.28	94.8	1217

3. RESULTS AND DISCUSSION

3.1. Process Simulation

A computational fluid dynamics simulation was carried out using the COMSOL Multi-Physics (version 5.2a, 2016) software wherein Figure 2 shows the mesh that was generated to effectively discretize the model. The regions of high mesh density (stratum corneum) coincide with regions that experience the greatest resistance to diffusion such as the Stratum corneum and highest concentration gradients (Richard, 2012). Concentration against time profiles were plotted at two points A and B representing the skin surface concentration and the blood concentration in the dermis respectively.

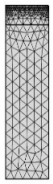

Figure 2: Mesh overview

Using the software and the theoretically developed models, a computational fluid dynamics simulation was carried out for a duration of 20 hours (72000seconds) with a time step of 100 seconds for a sample of crude oil with initial specific aromatic hydrocarbon concentration highlighted in their respective sections. The simulation gave rates of transfer of 7.234e^{-3} kg/m^3 for toluene, 5.341e^{-3} kg/m^3 for naphthalene, 2.854e^{-3} kg/m^3 for fluorene, and 1.310e^{-2} kg/m^3 for anthracene diffusing through the three layers of the fore arm skin of an adult male with the dimension of each layer given in Table 2.

Table 2: Estimated parameters from derived equations for various polycyclic aromatic hydrocarbon

Polycyclic aromatic hydrocarbon	$D_{Vehicle}$ $10^{-20}(m^2/s)$	$R_{Vehicle}$ $(kg/m^3.s)$	D_{SC} $10^{-15}(m^2/s)$	$D_{VE/D}$ $10^{-11}(m^2/s)$	K_E $10^{-7}(s^{-1})$
Toluene	6.173	31.843	5.192	7.445	2.981
Naphthalene	5.532	0.1146	8.881	3.542	7.029
Fluorene	5.071	9.969e-4	25.52	1.945	9.599
Anthracene	4.954	0.1393	23.25	1.036	7.255

3.1.1. Toluene

Toluene had an average concentration of 7.234x10^{-2} kg/m^3 and the diffusion coefficients of toluene in the vehicle, stratum corneum, viable epidermis and dermis were calculated to be 6.173x10^{-20} m^2/s, 5.192x10^{-15} m^2/s and 7.445x10^{-11} m^2/s respectively as shown in Table 2. Comparing the diffusion coefficient of the stratum corneum and the viable layers it can be seen that the stratum corneum has a lower diffusion coefficient which signifies a slower rate of transport in the stratum corneum, and as such, the rate controlling stage (Corie et al., 2020). The rate of evaporation was calculated to be 3.18425 $kg/m^3.s$ and the rate constant for the clearance into the blood stream through the dermis was 2.981e^{-7} s^{-1}. The simulations were ran for 72000 seconds and the 2D surface plot in Figure 3 was generated and shows a maximum concentration of toluene of 0.0853 kg/m^3 on the surface of the skin and the concentration of the compound reduces down the layers of the skin to a minimum concentration of 9.28x10^{-5} kg/m^3 in the dermis.

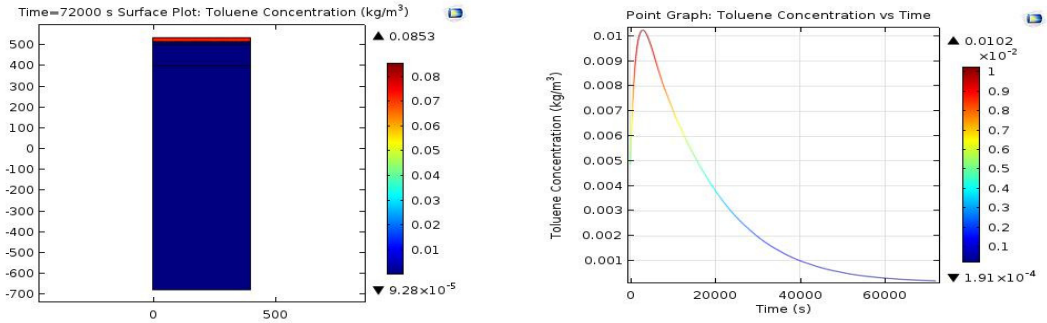

(a) (b)

Figure 3: 2D surface and toluene concentration versus time plot at point A

Figure 3 illustrate the concentrations of toluene in the topmost layer of the skin at different time intervals. The initial concentration at the stratum corneum is 0.0048537 kg/m^3. As time increases the SC gradually

becomes saturated with the compound and attains a maximum concentration of 0.010245 kg/m^3 at about 3000 seconds. As time progresses the concentration of toluene in the SC depletes as the compound diffuses down the deeper layers of the skin. The minimum concentration of toluene in the stratum corneum at 72000 seconds becomes 1.92x10^{-4} kg/m^3. The compound concentration rapidly increases initially due to high concentration gradients between the vehicle and the stratum corneum but begins to diffuse away slowly as time progressed. As the compound diffuses down the skin into the dermis and blood, its concentration profile at Point B is represented by Figure 4. From the graph, the compound is not initially present in the dermis but as time progresses the concentration of toluene in the blood increases till it attains a maximum concentration of 9.28e^{-5} kg/m^3 at 72000 seconds. The concentration of the compound increased over time, indicating that the compound was transferred to this location.

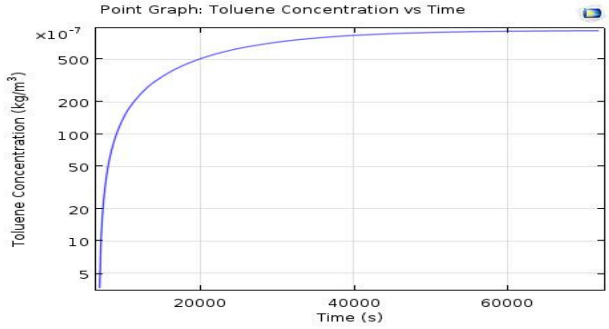

Figure 4: Toluene concentration with time plot at point B

3.1.1.1. Risk analysis for toluene

Toluene acts predominantly as a central nervous system depressant causing fatigue, headache, nausea, vertigo, muscular weakness, itching and burning of the skin. The threshold limit value (TLV) of toluene via dermal route according to both The National Institute for Occupational Safety and Health (NIOSH) and American Conference of Governmental Industrial Hygienists (ACGIH) is 100 ppm for exposure time of more than eight (8) hours (Masys and Vinegar, 2002). From Fig 4, the maximum concentration of toluene in the skin is 0.010245 kg/m^3 i.e. 10.245 ppm which is below the TLV and thus has no serious effects, just slight itching of the skin.

3.1.2. Naphthalene

From the polycyclic aromatic hydrocarbons studied, naphthalene had an average concentration of 5.341e^{-3} kg/m^3 and the diffusion coefficient of naphthalene in the vehicle, stratum corneum, viable epidermis and dermis were calculated to be 5.532x10^{-20} m^2/s, 8.881x10^{-15}m^2/s, and 3.542x10^{-11}m^2/s respectively as shown in Table 2. Comparing the diffusion coefficient of the stratum corneum and the viable layers it can be seen that the stratum corneum has a lower diffusion coefficient which signifies a slower rate of transport in the stratum corneum (Corie et al., 2020). The rate of evaporation was calculated to be 0.1146 kg/m^3.s, and the rate constant for removal of materials in the dermis was 7.029e^{-7} s^{-1}. Figure 5 shows a 2D surface and a concentration distribution plot. The 2D plot illustrates the concentrations of naphthalene in the system at 72000 seconds. From the plot at about 72000 seconds the maximum concentration of naphthalene is 6.21e^{-3} kg/m^3, which is at the surface of the skin or the vehicle and a minimum concentration of 6.64 x 10^{-6} kg/m^3 in the deeper layers of the skin. The concentration plot gives naphthalene concentrations at the top layer of the Stratum corneum at various times. Naphthalene concentration was initially 3.532e^{-4} kg/m^3, it increases drastically to attain a maximum concentration of 7.4494e^{-4} kg/m^3 in about 17000 seconds. On saturation the concentration gradually declines as the compound diffuses deeper into the skin layers, till it attains a minimum concentration of 6.68e^{-6} kg/m^3 at about 72000 seconds.

From Figure 6, the concentration of naphthalene in the lower dermis and blood was initially negligible, it increases till it attains a peak concentration of 6.74e^{-6} kg/m^3 at about 40700 seconds then gradually declines

due to blood clearance. The drug concentration increases, indicating the compound was transported to this location. The concentration the decrease after 40700 seconds, which indicates a gradual sink of the compound in this layer due to blood clearance.

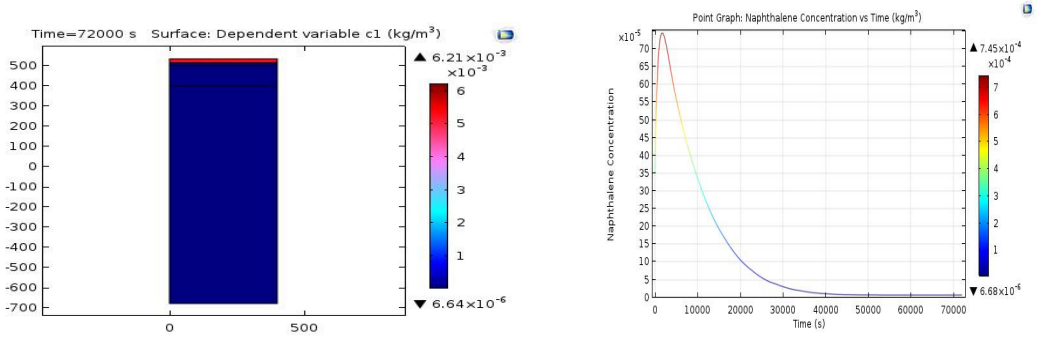

(a) (b)

Figure 5: 2D surface and naphthalene concentration versus time plot at point A

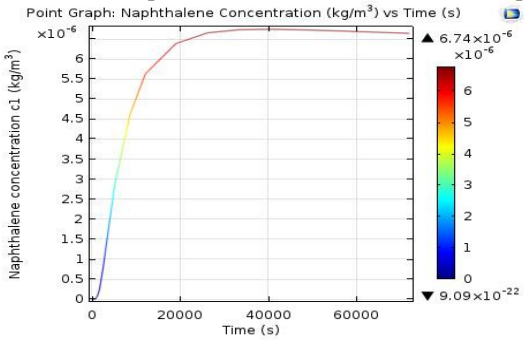

Figure 6: Naphthalene concentrations with time at Point B

3.1.2.1. Risk analysis for naphthalene

Naphthalene is carcinogenic and can affect humans via inhalation or dermal absorption. It causes headache, irritation of eyes, optical neuritis, corneal damage, nausea, vomiting, skin burns, dermatitis, profuse sweating, damage to the liver and kidney (haematuria (blood in the urine), irritation bladder). The Occupational Safety and Health Administration (OSHA) permissible exposure limit (PEL) and NIOSH recommended exposure limit (REL) for an eight-hour shift are both 10 ppm. From Figure 6, the maximum concentration of naphthalene in the skin is 7.4494e-4 kg/m^3 i.e. 0.74494 ppm leading to prolong sweating, headache, skin burns and dermatitis on exposures of over 24 hours. (OSHA, 2018)

3.1.3. Fluorene

Fluorene one of the polycyclic aromatic hydrocarbons studied, had an average concentration of 1.310e^{-2} kg/m^3 and the diffusion coefficient of fluorene in the vehicle, stratum corneum, viable epidermis and dermis were calculated to be 4.954 e^{-20} m^2/s, 2.325 e^{-14} m^2/s, and 1.036 e^{-11} m^2/s respectively. Comparing the diffusion coefficient of the stratum corneum and the viable layers it can be seen that the stratum corneum has a lower diffusion coefficient which signifies a slower rate of transport in the stratum corneum, as the stratum corneum presents the main barrier to transdermal diffusion. The rate of evaporation was calculated to be 9.969e^{-4} $kg/m^3.s$ and the rate constant for its removal in the dermis was 9.599e^{-7} s^{-1}.

Figure 7 show 2D surface and concentration distribution plot of Fluorene in the system at 72000 seconds. From the plot at about 72000 seconds the maximum concentration of Fluorene is 3.32e^{-3} kg/m^3, which is at the surface of the skin or the vehicle and a minimum concentration of 3.49e^{-6} kg/m^3 in the deeper layers of the skin.

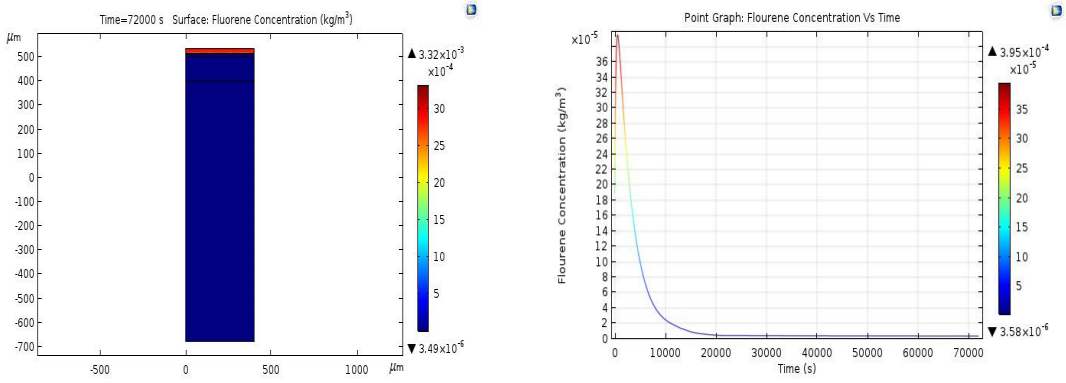

(a) (b)

Figure 7: 2D surface and fluorene concentration versus time plot at point A

The Figure illustrates the concentrations of fluorene in the topmost layer of the skin at different time intervals. The initial concentration of the top layer of the stratum corneum is 1.889e^{-4} kg/m^3. As time increases the SC rapidly becomes saturated with the compound and attains a maximum concentration of 3.95e^{-4} kg/m^3 at about 500 seconds. The compound concentration rapidly increases initially due to high concentration gradients between the vehicle and the stratum corneum. As time progresses the concentration of fluorene in the SC depletes as the compound diffuses down the deeper layers of the skin. The minimum concentration of toluene in the stratum corneum, which is at about 72000 seconds becomes 1.92e^{-4} kg/m^3. From Figure 8, the concentration of naphthalene in the lower dermis and blood was initially negligible, it increases till it attains a peak concentration of 3.522e^{-6} kg/m^3 at about 55000 seconds then gradually declines due to blood clearance in this layer. The compound concentration increases, indicating the compound was transported to this location.

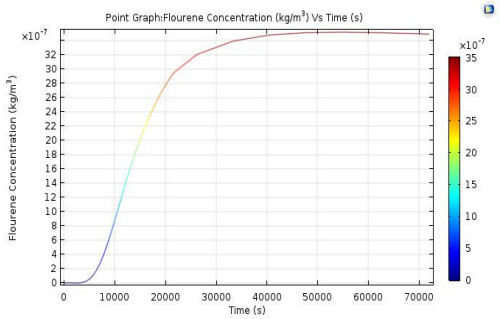

Figure 8: Graph showing fluorene concentration with time at point B

3.1.3.1. Risk analysis for fluorene

Fluorene has no known long-term chronic effect at this time but can cause erythema, dermal burns, skin and eyes irritations, thus prolonged contact must be prevented. (New Jersey Deparment of Health and Senior Services, 1999; Richard, 2012)

3.1.4. Anthracene

Anthracene from the study had an average concentration of 1.310e^{-2} kg/m^3 and the diffusion coefficient of Anthracene in the vehicle, stratum corneum, viable epidermis and dermis were calculated to be 5.071 e^{-20} m^2/s, 2.522 e^{-15} m^2/s, and 1.945 e^{-11} m^2/s respectively as shown in Table 2. Comparing the diffusion coefficient of the stratum corneum and the viable skin layers it can be seen that the stratum corneum has a lower diffusion coefficient which signifies a slower rate of transport in the stratum corneum, as the stratum

corneum presents the main barrier to transdermal diffusion. The rate of evaporation was calculated to be 0.1393 $kg/m^3.s$ and the rate constant for the drug removal in the dermis was 7.255e^{-7} s^{-1}.

Figure 9 show a 2D surface and concentration distribution plots illustrating the concentrations of naphthalene in the system at 72000 seconds. From the plot at about 72000 seconds the maximum concentration of naphthalene is 0.02 kg/m^3, which is at the surface of the skin or the vehicle and a minimum concentration of 1.6e^{-5} kg/m^3 in the deeper layers of the skin. The figure also shows Anthracene concentrations at the top layer of the Stratum corneum at various time intervals. Anthracene initial concentration of the stratum corneum is 8.674e^{-4} kg/m^3. As time increases the SC gradually becomes saturated with the compound and attains a maximum concentration of 0.00170031 kg/m^3 at about 700 seconds. As time progresses the concentration of toluene in the SC depletes as the compound diffuses down the deeper layers of the skin. The minimum concentration of anthracene in the stratum corneum at about 72000 seconds becomes 1.884e^{-5} kg/m^3. From Figure 10, the concentration of anthracene in the lower dermis and blood was initially negligible, it increases till it attains a peak concentration of 1.71e^{-5} kg/m^3 at about 72000 seconds. The compound's concentration increases, indicating the compound was transported to this location.

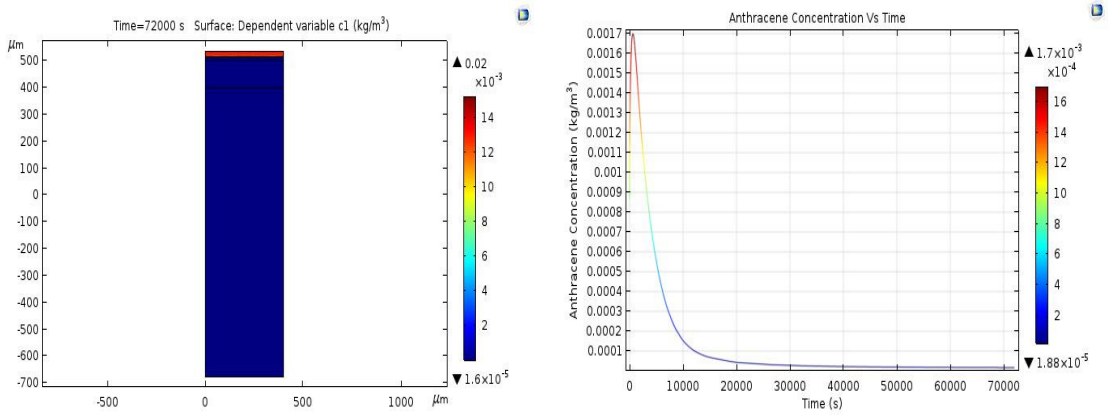

(a) (b)

Figure 9: 2D surface and anthracene concentration versus time plot at point A

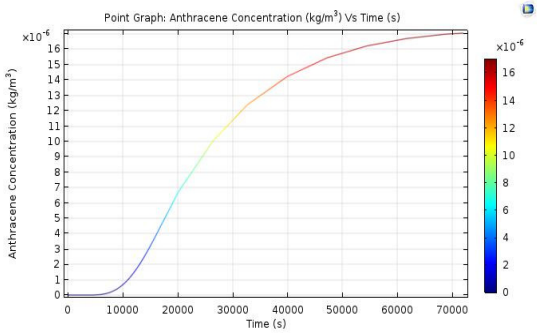

Figure 10: Anthracene concentration with time at point B

3.1.4.1. Risk analysis for anthracene

Anthracene is not a carcinogen but has detrimental effects on the skin like irritation, itching and inflammation which is aggravated by sunlight. Repeated contact can cause thickening of the skin, patchy areas of increased yellow-brown pigment changes and loss of skin pigment. The British Columbia Occupational Exposure Limit time weighted average (TWA) is 100 ppm for ten hours work time. From Figure 10 the maximum concentration of anthracene on the skin is 1.70031 ppm thus posing a considerably slow treat.

3.2. Sensitivity analysis

A sensitivity analysis was conducted with respect to the elimination rate constant and diffusion coefficients of the vehicle, stratum corneum and viable layers to examine how changes in these values on the model as shown in Figures 11 and 12. The value of each parameter was altered by $\pm 10\%$ while keeping other parameters constant and the maximum concentration of each compound in the blood was observed. Figure 12 show the sensitivity analysis on desired parameters that a change in the diffusion coefficient of the stratum corneum causes a very drastic change in the maximum concentration of the compounds in the blood, this is because the stratum corneum presents the major barrier or opposition to transdermal transfer (Flynn, 1990). The model is also very sensitive to the changes of the elimination or clearance rate constant as this tells how much of the compound diffuses into the blood stream as such cleared. From the sensitivity analysis on the diffusion coefficient of the vehicle it can be deducted that the vehicle diffusion coefficient has negligible effects to the maximum concentration of the compounds. Variations of the diffusion coefficient of the viable epidermis and the dermis show little effects to the maximum concentration of the compounds in the blood.

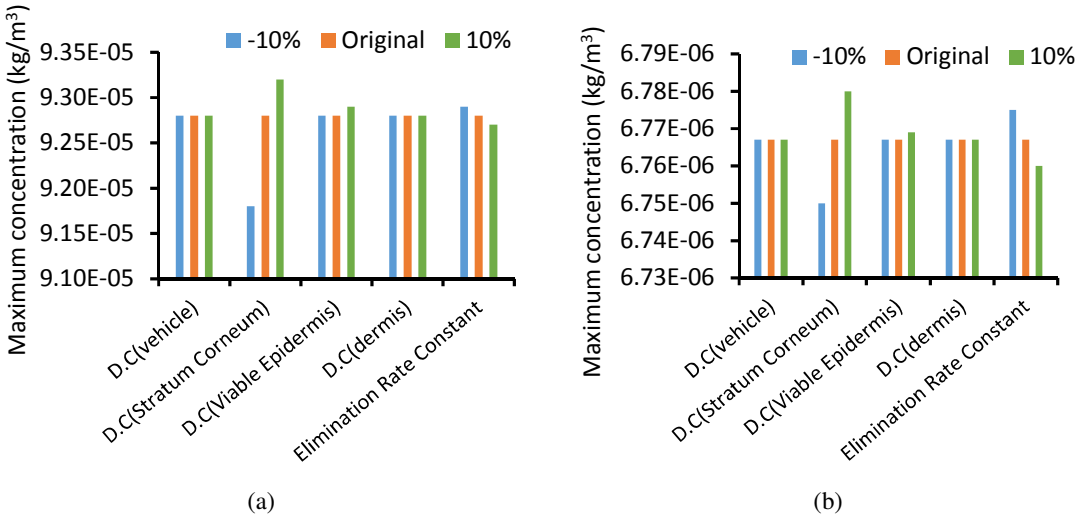

(a) (b)

Figure 11: Sensitivity analysis on toluene and naphthalene maximum blood concentration at point B

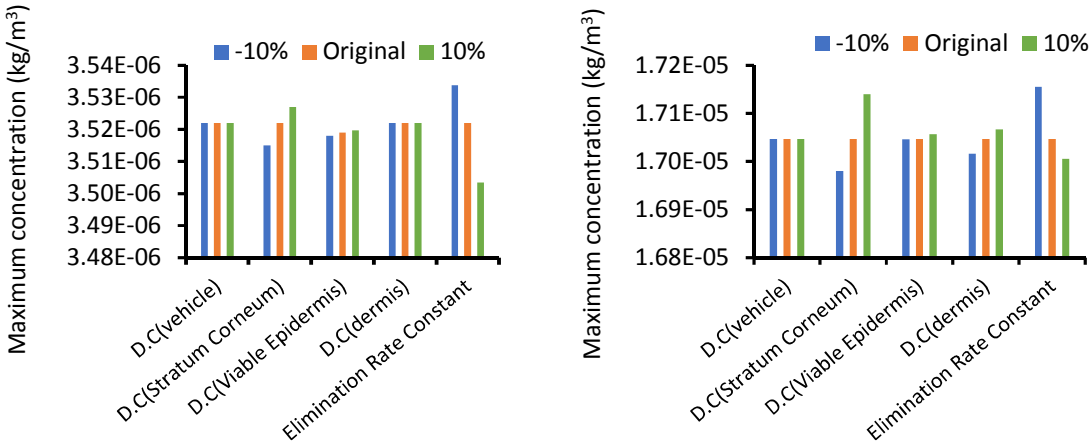

Figure 12: Sensitivity analysis on fluorene and anthracene maximum blood concentration at point B

4. CONCLUSION

Mathematical models based on the transport and diffusion of cyclic aromatic hydrocarbons through the various layers of the human skin were developed and also evaluated through a process simulation based on literature. Diffusion coefficient of the various cyclic aromatic hydrocarbons studied for the vehicle, stratum corneum, viable epidermis and dermis were calculated based on some level of detail regarding the modelling of the process using the Comsol multiphysics software. It was shown that the computational fluid dynamics simulation of the rate of transport for toluene, naphthalene, fluorine and anthracene for a duration of 20 hours through the three layers of the fore arm skin of an adult male under different operating conditions gave 7.234e-3 kg/m^3, 5.341e^{-3} kg/m^3, 2.854e^{-3} kg/m^3, and 1.310e^{-2} kg/m^3 respectively for the average concentration of the PAHs after the process. Risk analysis were performed for all the PAHs studied and their health effects observed. Sensitivity analysis was also carried out on all the estimated parameters and the stratum corneum was shown to be the most sensitive parameter, and this is in accordance with literature**.**

5. CONFLICT OF INTEREST

There is no conflict of interest associated with this work.

REFERENCES

Almad, R. G., Nor, F.R., Mohammad, F. Z., Nazeha, A. and Omchit, S. (2021). Assessment of skin irritation and sensitization effect by tropical Ptorostilbene. Biomedical and Pharmacology Journal, 14(4), pp. 1917-1927

Anissimov, Y. G., and Roberts, M. S. (2011). Modelling Dermal Drug Distribution After Topical Application in Human. *Journal of Pharmaceutical Research, 28*, pp. 2119–2129.

Carroll, R., and Abdel-Rahman, A. (2007). Regulation of Acid-Base Balance. *The Comprehensive Pharmacology Reference., 2*, pp. 1–2

Chen, L., Han, L., Saib, O., and Lian, G. (2015). In Silico Prediction of Percutaneous Absorption and Disposition Kinetics of Chemicals. *Journal of Pharmaceutical Research, 32*, pp. 1779–1793.

Chen, L., Lian, G., and Han, L. (2010). Modeling Transdermal Permeation . Part I . Predicting Skin Permeability of Both Hydrophobic and Hydrophilic Solutes. *Journal of Pharmaceutical Research, 12*, pp. 56

Corie, A. E, Kelvin, O., Tankersley, C. M., Obringer, G. J., Carr, J. M., Helga, R., Helene, D., Camlle, G., Sebastien, G., Nicola, J., Hewitt, C. J. J., Martina, K., Daniela, L., Alexandra, R. and Andreas, S. (2020). Partition coefficient determination of 50 compounds in human intact skin, isolated skin layers and isolated stratum corneum lipids. Toxicology in Vitro.8, pp. 43-51.

Crank, J. (1975). *The Mathematics of Diffusion* (2nd ed.). Oxford: Clarendon Press. pp. 54.

Dancik, Y., Matthew, A., Miler, J. J. and Gerald, B.K. (2013). Design and Performance of a spreadsheet model for estimating bioavailability of Chemicals from dermal exposure. Advance Drug Delivery Reviews, 65, pp. 221-236

Dominik, S., Dirk, N. and Ulrich, F. S. (2015). Mathematical Models for Dermal drug absorption, Article in: Expert opinion on Drug Metabolism and toxicology, 30, pp. 64-72.

Flynn, G. L. (1990). Physicochemical determinants of skin absorption. Princ. route-to-route extrapolation risk Assess. pp. 93–127.

Fu, X.C., Wang,G.P., Wang, Y.F., Liang, W.Q., Yu, Q.S., Chow, M.S.S (2004). Limitations of the Potts and Guy's model and a predictictive algorithm for skin permeamility including the effects of hydrogen-bond on diffusivity. International Journal of Pharmaceutical Sciences, 59(4), pp. 282-285

Ibrahim, R. and Kasting, G. (2010). Improved Method for Determining Partition and Diffusion Coefficients in Human Dermis. *Journal of Pharmacuetical Science, 99*, pp. 4928–4939.

Jane, R. and Jane, L. (2003). *Qualitative Research Practice:* A Guide for Social Science Students and Researchers*., 5* (4), pp. 336

Kasting, G. B. and Miller, M. A. (2006). Kinetics of Finite Dose Absorption through Skin for Volatile Compounds. *Journal Pharmacuetical Science., 95*, pp. 268–280.

Kretsos, K., Miller, M., Zamora-Estrada, G., and Kasting, G. (2008). Partitioning, diffusivity and clearance of skin permeants in mammalian dermis. *International Journal of Pharmaceutics, 346*, pp. 64–79.

Laurnent, S. (2022). Analysis of the absorption kinetics following dermal exposure to large doses of volatile organic compounds. Mathematical Biosciences, 35 (1), pp. 108889

Lee, Y., and Hwang, K. (2002). Skin thickness of Korean adults. . Journal of *Surgical and Radiologic Anatomy, 24*, pp. 183–189.

Lee, Y., Kim, H., Pham, Q., Lee, J., and Kim, K. (2022). Pharmacokinetics and the Dermal Absorption of Bromochlorophene, a cosmetic preservative ingredient. Toxics, 10, pp.329

Masys, D. A. and Vinegar, A. (2002). *Health effects of crude oil exposure..Jounal of* Ohio Naval medical reserch institue, 4, pp.26-32

Mccarley, K., and Bunge, A. (2001). Pharmacokinetic models of dermal absorption. *Journal Pharmaceutical Science, 90*, pp. 1699–1719.

Neha, G., Purva, T. and Bharti, S. (2017). Surging footprints of mathematical modeling for prediction of transdermal permeability. *Asian journal of pharmaceutical sciences, 12 (14), pp.* 299–325.

New Jersey Deparment of Health and Senior Services (1999). Flourene. *Hazardous Case Fact Sheet*, pp. 1-6.

OSHA . (2018, January 2). *NIOSH: OSHA1998*. Retrieved from Central for Disease Pontrol and Prevention: https://www.cdc.gov/niosh/pel88/91-20.html

Rania, I., Nitsche, J., and Gerald, B. K, (2012.). Dermal Clearance Model for Epidermal Bioavailability Calculations, *Journal of Pharmaceutical Science, 101* (6), pp. 2094–2108.

Richard, P. P. (2012). *Sittig's Handbook of Toxic and Hazardous Chemicals and Carcinogens*. Oxford: Elsevier.

Saranya, K., Maddela, Naga, R., Megharaj, M., Venkateswarlu, K. (2020), Impact of total petroleum hydrocarbons on human health. In book: Total Petroleum Hydrocarbons, pp.6.

Scheuplein, R., and Bronaugh, R. (1983). Percutaneous absorption. *ochemistry Physiol. Ski., 2*, 1255–1295.

US EPA (1981). Mathematical models for estimating workplace concentration levels, a literature review; (EPA contract 88-01-6065-ed). Clement Associates.

Won, H., Jeong, D.H., Shin, H.S., Lee, J.H., Lee, J.P., Yang, J.Y., Jung, K., Jeong, J., Oh, J.H.(2021). Toxicological Assessment of Bromochlorophene: Single and Repeated-Dose 28-Day Oral Toxicity, Genotoxicity, and Dermal Application in Sprague-Dawley Rats. Frontiers in Pharmacology. Volume 12, issue 690141.